ELSEVIER

Journal of Biomechanics 39 (2006) 2476–2483

JOURNAL OF BIOMECHANICS

www.elsevier.com/locate/jbiomech
www.JBiomech.com

Finite element modelling of glenohumeral kinematics following total shoulder arthroplasty

Andrew R. Hopkins[a], Ulrich N. Hansen[a,*], Andrew A. Amis[a,b], Mark Taylor[c], Nicole Gronau[d], Carolyn Anglin[e]

[a]Biomechanics Section, Mechanical Engineering Department, Imperial College London, Room 636, Mechanical Engineering Building, South Kensington Campus, London SW7 2AZ, UK
[b]Musculoskeletal Surgery Department, Imperial College London, London, UK
[c]Bioengineering Science Research Group, School of Engineering Sciences, University of Southampton, Highfield, Southampton, UK
[d]Department of Biomechanics, Zimmer GmbH, Winterthur, Switzerland
[e]Department of Mechanical Engineering, University of British Columbia, Vancouver, Canada

Accepted 22 July 2005

Abstract

Due to the shallowness of the glenohumeral joint, a challenging but essential requirement of a glenohumeral prosthesis is the prevention of joint dislocation. Weak glenoid bone stock and frequent dysfunction of the rotator cuff, both of which are common with rheumatoid arthritis, make it particularly difficult to achieve this design goal. Although a variety of prosthetic designs are commercially available only a few experimental studies have investigated the kinematics and dislocation characteristics of design variations. Analytical or numerical methods, which are predictive and more cost-effective, are, apart from simple rigid-body analyses, non-existent.

The current investigation presents the results of a finite element analysis of the kinematics of a total shoulder joint validated using recently published experimental data for the same prostheses. The finite element model determined the loading required to dislocate the humeral head, and the corresponding translations, to within 4% of the experimental data. The finite element method compared dramatically better to the experimental data (mean difference = 2.9%) than did rigid-body predictions (mean difference = 37%). The goal of this study was to develop an accurate method that in future studies can be used for further investigations of the effect of design parameters on dislocation, particularly in the case of a dysfunctional rotator cuff. Inherently, the method also evaluates the glenoid fixation stresses in the relatively weak glenoid bone stock. Hence, design characteristics can be simultaneously optimised against dislocation as well as glenoid loosening.

Keywords: Total shoulder arthroplasty; Finite element analysis; Subluxation

1. Introduction

Ensuring proper muscle tensions and balancing of the shoulder joint during total joint replacement surgery is essential for improving function and relieving pain (Neer et al., 1982; Laurence, 1991; Wirth and Rockwood, 1996). Particularly in cases where the rotator cuff is dysfunctional, the risk of recurrent subluxation or dislocation of the shoulder is very high (Moeckel et al., 1993). Hasan et al. (2002), reported that in 35% of cases referred for revision arthroplasty, joint instability was the primary indicator, which is also evident in other literature (Wirth and Rockwood, 1996; Oosterom et al., 2003). Where the rotator cuff is deficient, alterations to the prosthesis design may provide a remedy. Two important design parameters which affect the stability and kinematics of the prosthesis are glenohumeral

*Corresponding author. Tel.: +44 0 207 594 7061.
E-mail address: u.Hansen@imperial.ac.uk (U.N. Hansen).

0021-9290/$ - see front matter
doi:10.1016/j.jbiomech.2005.07.031

conformity (i.e. the ratio of humeral head and glenoid radii) and constraint (i.e. the maximum slope of the glenoid articular rim), as demonstrated in Fig. 1. The design can theoretically be tailored to achieve required kinematic behaviour and thereby accommodate for deficiencies of the soft tissues. Specifically, very constrained designs are in principle desirable to improve stability in cases of a dysfunctional rotator cuff. However, the design process is not straightforward, as highlighted by the high failure rates of these very constrained designs (Wirth and Rockwood, 1996). Although in principle offering high resistance to subluxation they also generated relatively high-fixation stresses in the weak glenoid bone. Walch et al. (2002) recently identified a significant linear relationship between the glenoumeral radial mismatch and a measured glenoid radiological score (radiolucencies surrounding the prosthesis), with the best results seen for mismatches greater than 5.5 mm, with no related increase in clinical instability. However, a study by Karduna et al. (1997) showed that relatively low conformity design (3–5 mm mismatch) mimic the normal glenohumeral kinematics best.

Experimental studies have examined the effect of implant conformity and constraint on subluxation loads and intra-articular joint translations (Severt et al., 1993; Anglin et al., 2000), however, the associated materials and labour costs are often high. In an effort to mitigate the costs of repeated testing, and following the work of Karduna et al. (1997) and Walker et al. (1995), Anglin et al. (2000) presented rigid-body analyses to help predict subluxation loads and translations of the glenohumeral joint during loading, which were later compared with experiments for the purpose of validation. In comparison, the rigid-body analysis overestimated the subluxation loads typically by 20–50%, which was suggested to be caused by the inability of the rigid-body models to account for prosthesis deformation under loading. More sophisticated finite element techniques, as with rigid-body analyses, provide cost effective alternatives to laboratory testing and also create a framework for understanding the results on a theoretical basis (Oosterom et al., 2003). Additionally, finite element models provide estimates of joint contact pressures, material deformation and fixation stresses that are difficult, if not impossible, to obtain using laboratory tests. Furthermore, one can easily and relatively quickly repeat the analyses for both small and large variations in the design parameters, allowing for a more complete understanding of their relative effects.

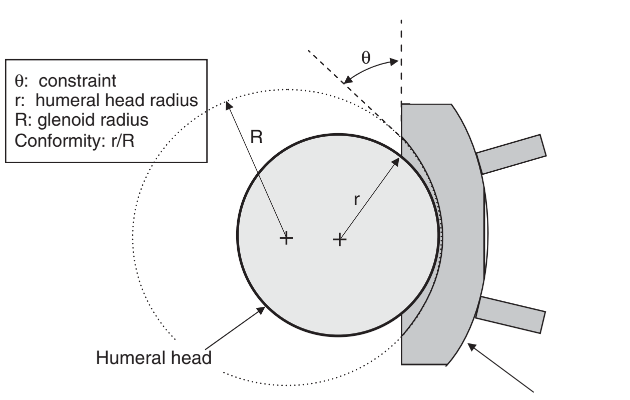

Fig. 1. Definition of conformity (i.e. ratio of humeral head radius over glenoid radius) and constraint (i.e. the maximum slope of the glenoid articular rim) in the glenohumeral joint.

Indeed, the finite element method has been used in several studies of the glenohumeral joint over the last decade. However, in none of those previous studies was the method used for investigating the effects of implant design on subluxation loads or glenohumeral joint kinematics. The 'standard' type of finite element method used in orthopaedic biomechanics treats a problem as quasi-static. Typically, if the simulation involves contact it is solved as a series of static problems where the solution is updated as the contact condition is developing. Following this approach, the governing equations that need to be solved for displacement $\{\delta\}$ within each step of the developing contact are $[K]\{\delta\} = \{F\}$ where $[K]$ is the stiffness matrix of the system and $\{F\}$ represents the applied forces. Solution of this system involves triangularizing a large stiffness matrix and is very costly in terms of computer resources. This technique is often referred to as an implicit formulation.

An alternative approach is a so-called explicit finite element method. This method treats the problem as a dynamic time-dependent problem with the governing dynamic equations $[M]\{\ddot{\delta}\} + [C]\{\dot{\delta}\} + [K]\{\delta\} = \{F\}$. In this equation $(\cdot)$ indicates the time derivative and $[M]$ and $[C]$ are, respectively, the mass and damping matrices of the system. The mass and damping matrices can be given very low values so that inertia and damping will have negligible effect on the calculated $\{\delta\}$ and effectively the explicit method simply represents an alternative method for solving the static problem. These pseudo-dynamic equations are solved from an initial known condition through a series of incremental time steps. Using a central difference method to integrate the equations over time, $\{\delta\}$ can be calculated without having to triangularise large matrices and the method can, for some problems, be much faster than the standard method.

In a previous work related to the kinematics of the knee joint it was found that the standard implicit formulation was resulted in extremely long solution times (Godest et al., 2002). Therefore, the standard formulation was deemed impractical for predicting the kinematics of contacting articulating joints, possibly explaining why the method has never been used for predicting glenohumeral joint kinematics. However, Godest et al. (2002) was able to demonstrate accurate predictions of kinematics of a total knee joint replacement, using the explicit finite element formulation, validated against the motions exhibited by the Stanmore knee wear simulator. Therefore, the explicit finite element formulation has been adapted within the current study to evaluate the method's capacity for predicting subluxation-related kinematics of the glenohumeral joint. This report shall demonstrate the applicability of explicit finite element analysis to modelling of the total shoulder replacement, through comparison with previously published experimental data.

2. Methods

Anglin et al. (2000) investigated the effects of glenoid component designs on the forces required to cause subluxation of the humeral head. An experimental testing apparatus was used and several different commercial component designs were tested in order to determine their ability to withstand dislocation. These prostheses were mounted within a polyurethane substrate block with material properties similar to glenoid cancellous bone (Anglin et al., 1999). Compressive loading of 750 N was applied through the humeral head towards the centre of the glenoid component and followed by a shearing translation, which was increased linearly until humeral subluxation. This testing method has since been adopted as a standard for glenoid component testing (ASTM F2028-00). Rigid-body analysis of the glenohumeral interaction was performed in order to gauge the effects of design parameters on dislocation forces and corresponding humeral translations.

Validation of the finite element models shall be achieved through direct comparison with the results of the cited experimental model. Finite element models of four different glenoid components tested in the experimental study were generated from CAD data provided by Zimmer GmbH (seen in Fig. 2). Details regarding the characteristics of the different meshes can be found in Table 1. Data regarding the prostheses' geometry and the loading required to induce subluxation of the humeral head, as developed in the experimental model and through rigid-body predictions, are presented in Table 2. An example of the final finite element models simulating the experimental set-up including a polyurethane mounting block, is presented in Fig. 3. The faces of the polyurethane were constrained from moving, and the interfaces between the implant/cement and cement/polyurethane were modelled as rigid.

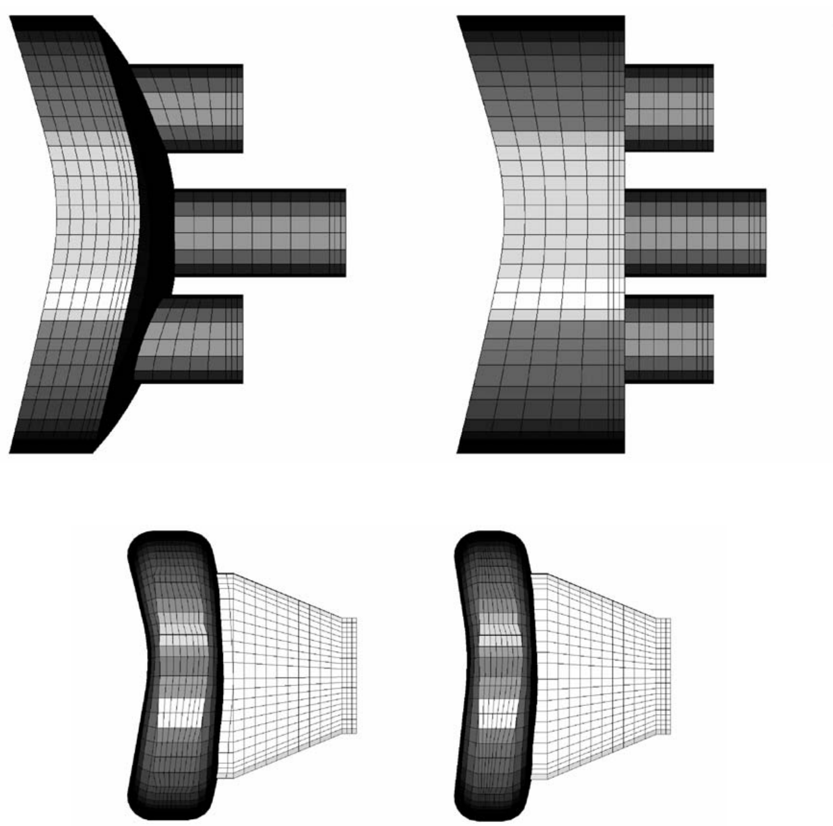

Fig. 2. Finite element models of the four glenoid component designs. Top left, pegged curved–backed size *L*; top right, pegged flat-backed size *L*; bottom left, keeled conforming size XS; bottom right, keeled non-conforming size XS.

Table 1
Details of number of elements in meshes used for subluxation models

Glenoid design	Polyethylene	Cement	Polyurethane
Pegged curve-backed, size *L*	13,068	5914	32,894
Pegged flat-backed, size *L*	13,068	5914	35,565
Keeled non-conforming, size XS	5198	4938	31,267
Keeled conforming, size XS	5198	4938	31,267

Table 2
Geometric details of glenoid components used for FEA study of humeral head dislocation

Glenoid Design	Pegged curved-backed	Pegged flat-backed	Keeled conforming	Keeled non-conforming
Glenoid radius, R	29.5 mm	29.5 mm	20.5 mm	31.8 mm
Humeral radius, r	26 mm	26 mm	20 mm	20 mm
Conformity $= r/R$	0.88	0.88	0.98	0.63
Constraint	43°	43°	38°	25°
Rigid-body prediction	795 N	795 N	667.5	405 N
Experimental load	540 N	532.5 N	510 N	337.5 N

Rigid-body and average experimental loads to subluxation also presented (Anglin et al., 2000).

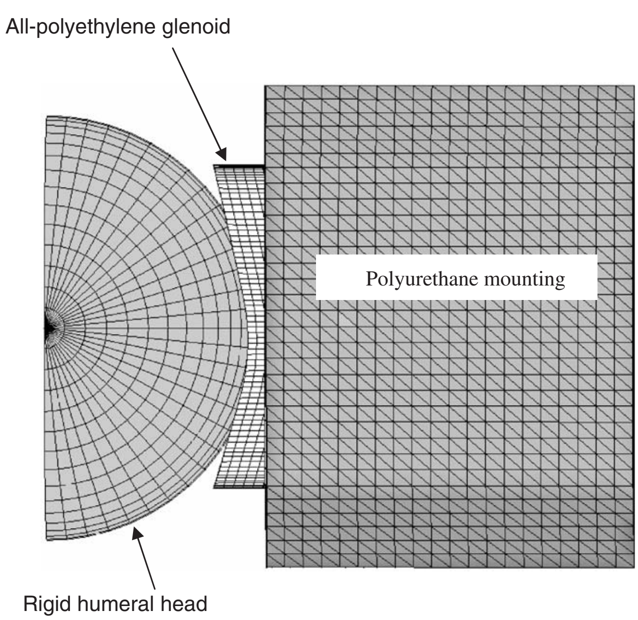

Fig. 3. Example FE model used to evaluate subluxation load and translation.

The material properties of the SULENE UHMWPE glenoid components were provided by the manufacturer, with the Young's modulus set to 1.26 GPa at 20 °C (Internal report—Centerpulse Orthopedics Ltd., M6470), a Poisson's ratio of 0.4 and a yield strength of 21 MPa. Young's modulus and Poisson's ratios of the PMMA bone cement were set at 2 GPa and 0.23, respectively (Friedman et al., 1992; Stone et al., 1999). Loading from the humeral component was provided through a rigid spherical shell model, and following the experimental protocol no humeral head rotation was permitted. The polyurethane bone substitute was assigned a Young's modulus of 0.193 GPa, following data provided by the foam manufacturers (Anglin et al., 2000). A coefficient of friction of 0.07 was assumed as reported by Anglin et al. (2000), who carried out friction tests for this particular material coupling and under conditions similar to the subluxation testing.

The explicit finite element solver PAM-SAFE (ESI Group, Paris, France) was used to perform the analyses. PAM-SAFE uses a contact penalty algorithm. An assessment of the sensitivity of the models to the effects of mesh density, penalty factor, contact zone thickness, inertia and the size of the incremental time-step ensured that the chosen settings of these parameters did not create numerical artefacts in the predicted subluxation loads and kinematics (Hopkins, 2004). However, to ensure that a stable contact was established at the glenohumeral joint a maximum time-step size of 3×10^{-3} s was identified for this particular analysis.

Often the terms stability, subluxation and dislocation are used interchangeably leading to confusion. In this paper we basically use the terminology also described by Oosterom et al. (2003). Referring to Fig. 4 the analysis starts with the humeral head centred in the glenoid cavity with the resultant force directed horizontally. As the humeral head moves superiorly the resultant force becomes increasingly vertical. As long as the force is directed into the glenoid cavity, moving the humeral head further superiorly requires a larger vertical force and the joint is therefore considered stable. When the humeral head is in contact with only the rim of the glenoid (Fig. 4, middle) the resultant force is only just pointing into the glenoid cavity. Further vertical

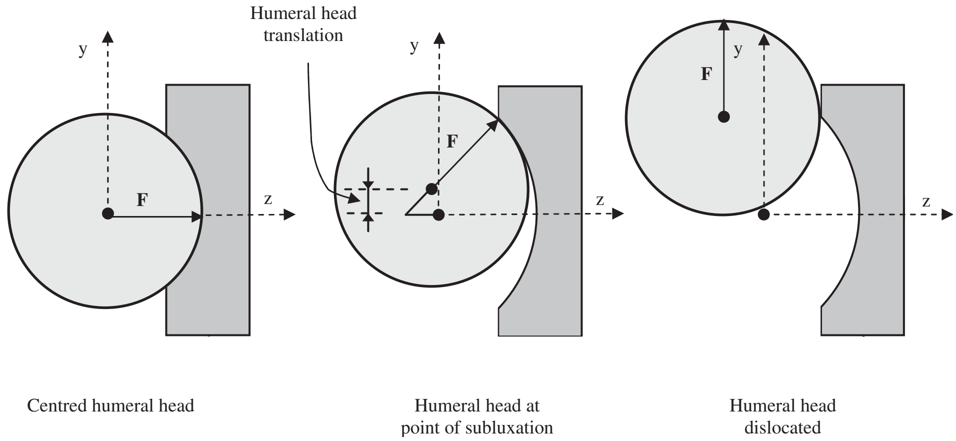

Fig. 4. Definition of subluxation, dislocation and humeral head translation used in this study. 'F' in the figure indicates the orientation of the joint force. Humeral head translation reported in this study is humeral head translation to initiation of subluxation as indicated in the middle figure.

movement will result in the resultant force pointing outside the cavity. To move the humeral head up further from this position still requires a vertical force but the maximum vertical force is reached at this position. Therefore, if the vertical force is increased or just maintained the middle position in Fig. 4 indicates a point of instability and we refer to this position as the point at which 'subluxation' is initiated. Under physiological conditions the muscles will probably at least maintain the vertical load and the humeral head will therefore 'jump' to the third position on the right sketch of Fig. 4 unless the capsule or passive muscle bulk constrain the humeral head from moving further. This third position is referred to as 'dislocation' and is characterised by virtually no resistance to further vertical movement. As the dislocated position offers no resistance to any vertical movement this position is of course very unstable. However, as described above instability is initiated at the subluxed position and it is therefore this position that needs to be understood and ultimately prevented.

A constant axial compressive load of 750 N was applied to the model and an increasing vertical (superior) shearing component was introduced linearly to the point of humeral subluxation. The humerus was permitted to translate through all three axes, but not to rotate, following the experimental set-up. Results shall be presented in the form of force ratios, these being the ratio of the maximum vertical force over the applied compressive force.

3. Results

The translation of the humeral head was monitored during loading and was recorded to the point of subluxation (Fig. 4, middle). At this point the amount of vertical loading was also recorded. A comparison of the force ratios required to dislocate the humeral head, obtained from the finite element models versus the experimental data and rigid-body predictions (Anglin et al., 2000) is presented in Fig. 5. As seen from this figure the finite element predictions compare remarkably well with the experimental results; mean and maximum difference of 2.9% and 4.4%, respectively. Rigid-body predictions over-predicted the experimental results by a mean and maximum difference of 37% and 49%, respectively. Rigid-body predictions were poorest for implants with large force ratios suggesting that polyethylene deformation influences the subluxation force. As verification of the numerical implementation of the explicit finite element method, the stiffness and yield strength of each of the materials were increased to values well above the real values quoted earlier, thus approximating the rigid-body analysis. Indeed, at stiffness values one thousand times their real values the difference between dislocation force ratios predicted by the rigid-body analysis and the finite element method was between 2% and 12% (see Fig. 5), a result that provides additional confidence in the numerical implementation. The translations of the humeral head are presented in Fig. 6. The finite element predictions again compared very well with the experimental data (mean and maximum difference of 3.8% and 8.8%, respectively) while the rigid-body analysis significantly under-predicted the translations (mean and maximum difference of 46% and 82%, respectively).

From the results, it was clear that high constraint leads to high force ratios and low conformity leads to large humeral head translations. However, due to the limited number of samples taken in this study only qualitative data can be presented on these trends at this time and the delineation of these parameters is currently being investigated in a parallel study aimed specifically at the effect of conformity and constraint on glenohumeral kinematics.

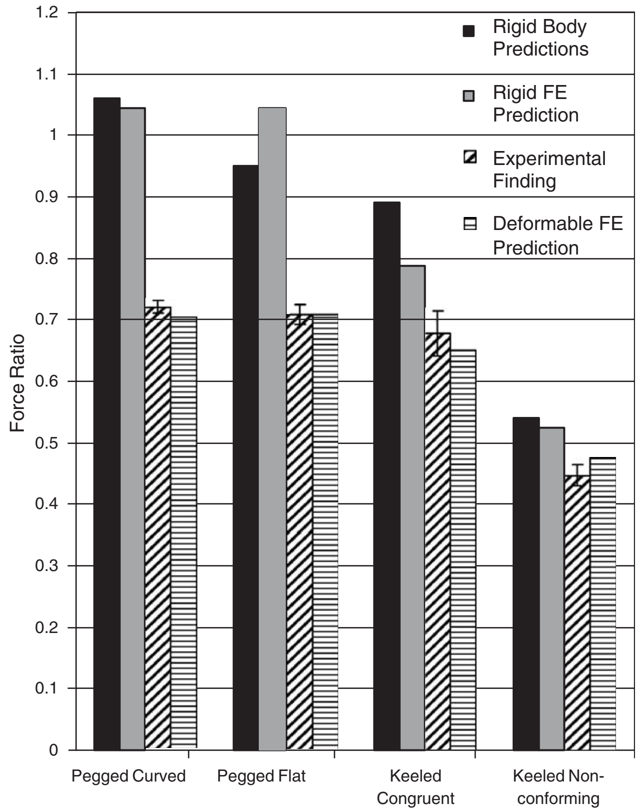

Fig. 5. Force ratio analysis (maximum vertical subluxation-force over the applied horizontal force). Graph displays experimental, $n = 2$, (including range of results), rigid-body and FEA results for the four components.

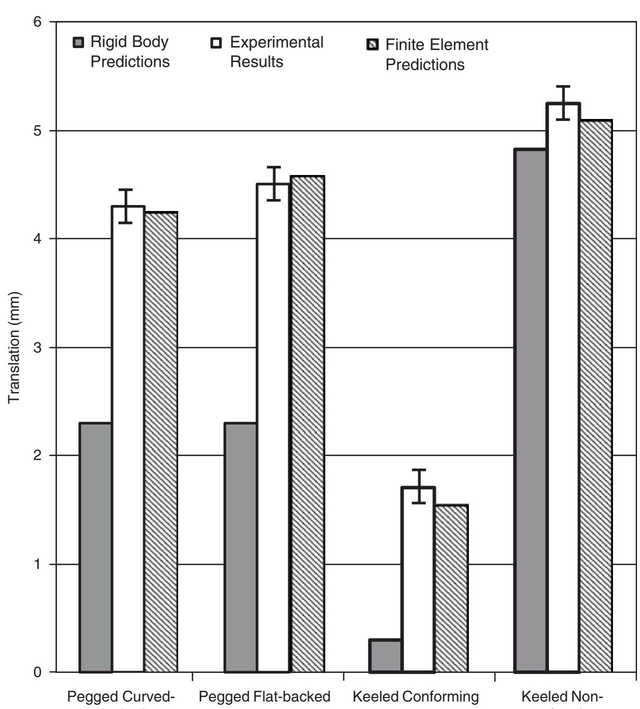

Fig. 6. Results of humeral head subluxation translations. Graph displays rigid-body, experimental, $n = 2$, (including range of results) and FEA results for the four components.

4. Discussion

Explicit time-stepping schemes in finite element analysis have recently been introduced by several groups in an attempt to more accurately model the kinematics of prosthetic joints. Successful early efforts on the artificial knee by Godest et al. have been followed up and further developed into effective predictive tools by several groups (Penrose et al., 2002; Halloran et al., 2005). However, the application of these techniques to the artificial shoulder had not yet, to the author's knowledge, been attempted. In this study, finite element simulations of the testing apparatus presented by Anglin et al. (2000), showed very good correlation with experimental subluxation force ratios for four different glenoid designs. Humeral head translations and subluxation forces were calculated far more accurately using FEA than rigid-body hand calculations. All predicted subluxation forces and translations were within the narrow range of the data presented in the experimental study. The high correlation between the observed simulation and experimental data, as well as the very small variation of the experimentally determined force ratios, indicate that dislocation is dominated by global parameters such as implant design, surgical alignment and material stiffness, as opposed to local phenomena such as material failure.

The finite element predictions confirmed that prosthesis constraint and conformity are two key implant design characteristics that dominate dislocation load and humeral head translation, respectively. Albeit this study never intended to provide an exhaustive investigation of various designs, it seems clear that other design features such as pegged or keeled designs have little direct influence on dislocation loads or kinematics. However, efforts to improve the fixation strength of the glenoid will of course allow for increased levels of prosthesis constraint and, hence, ultimately will provide a more dislocation resistant implant. In the current study the internal interfaces were modelled as rigid, whereas much evidence exists in the literature that suggests that the bonding between PMMA and polyethylene is less perfect. However, a later experimental study conducted by Anglin et al. (2001) noted that during the first few instances of loading the glenoid remained well seated within the polyurethane, and was only noted to 'distract' when in excess of 100,000 cyclic loads were applied.

Large polyethylene deformation was noted to occur at the point of dislocation, as shown in Fig. 7, confirming the result by Anglin et al. who showed that the deformation of the glenoid component itself and not the polyurethane backing material had the greatest influence on the predicted loads and kinematics. Furthermore, and as mentioned earlier, when the polyethylene modulus was increased by a factor of 1000, thus essentially simulating a rigid-body, finite

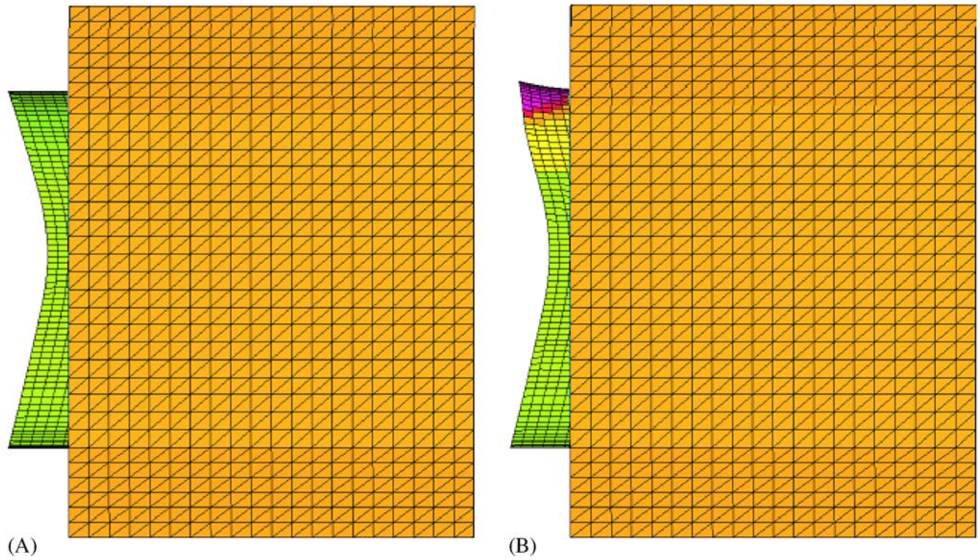

Fig. 7. Example of polyethylene deformation developed under loading. (A) initial state of model; (B) superior deformation of UHMWPE at point of humeral subluxation.

element predictions approached those presented by rigid-body analysis. Therefore, the results confirm Anglin et al.'s experimental observations of polyethylene deformation and the hypothesis that this is the reason for the failure of the rigid-body predictions.

By comparison with a parallel experimental study this investigation has validated the explicit finite element method and demonstrated its use as an effective predictive tool with regards to assessing the relationships between glenoid design and shoulder kinematics. Having established the finite element tool, the technique is currently being employed in more extensive studies of the effects of congruency and constraint, particularly addressing optimal implant characteristics in connection with a dysfunctional rotator cuff. The technique will also be a very useful tool in studies addressing that most challenging task of optimising, not only for joint dislocation but simultaneously also for glenoid loosening. Perhaps most immediately practical in regard to loosening, the subluxation translation is required in order to perform the experimental glenoid loosening test described in ASTM F2028-00. It would be very beneficial to determine this distance numerically rather than experimentally.

Acknowledgements

This work was supported by EPSRC Grant GR/N24681/01, EPSRC Award 00305929 and the University of London Central Research Fund.

References

Anglin, C., Tolhurst, P., Wyss, U.P., et al., 1999. Glenoid cancellous bone strength and modulus. Journal of Biomechanics 32, 1091–1097.

Anglin, C., Wyss, U.P., Pichora, D.R., 2000. Shoulder prosthesis subluxation: theory and experiment. Journal of Shoulder and Elbow Surgery 9 (2), 104–114.

Anglin, C., Wyss, U.P., Nyffeler, R.W., et al., 2001. Loosening performance of cemented glenoid prosthesis design pairs. Clinical Biomechanics 16, 144–150.

Friedman, R.J., LaBerge, M., Dooley, R.L., et al., 1992. Finite element modeling of the glenoid component: effect of design parameters on stress distribution. Journal of Shoulder and Elbow Surgery 1 (5), 261–270.

Godest, A.C., Beaugonin, M., Haug, E., et al., 2002. Simulation of knee joint replacement during a gait cycle using explicit finite element analysis. Journal of Biomechanics 35, 267–275.

Halloran, J.P., Petrella, A.J., Rullkoetter, P.J., 2005. Explicit finite element modeling of total knee replacement mechanics. Journal of Biomechanics 38, 323–331.

Hasan, S.S., Leith, J.M., Campbell, B., et al., 2002. Characteristics of unsatisfactory shoulder arthroplasties. Journal of Shoulder and Elbow Surgery 11 (5), 431–441.

Hopkins, A.R., 2004. Total Shoulder Arthroplasty Simulation using Finite Element Analysis, Ph.D. Thesis, Department of Mechanical Engineering, Imperial College London.

Karduna, A.R., Williams, G.R., Williams, J.L., et al., 1997. Glenohumeral joint translations before and after total shoulder arthroplasty. A study in Cadavera. Journal of Bone and Joint Surgery 79 (8), 1166–1174.

Laurence, M., 1991. Replacement arthroplasty of the rotator cuff deficient shoulder. Journal of Bone and Joint Surgery 73B, 916–919.

Moeckel, B.H., Altchek, D.W., Warren, R.F., et al., 1993. Instability of the shoulder after arthroplasty. Journal of Bone and Joint Surgery 75A (4), 492–497.

Neer, C.S., Watson, K.C., Stanton, F.J., 1982. Recent experiences in total shoulder replacement. Journal of Bone and Joint Surgery 64A (3), 319–337.

Oosterom, R., Herder, J.L., van der Helm, F.C.T., et al., 2003. Translational stiffness of the replaced shoulder joint. Journal of Biomechanics 36, 1897–1907.

Penrose, J.M.T., Holt, G.M., Beaugonin, M., et al., 2002. Development of an accurate three-dimensional finite element knee model.

Computer Methods in Biomechanics and Biomedical Engineering 4 (4), 291–300.

Severt, R., Thomas, B.J., Tsenter, M.J., et al., 1993. The Influence of conformity and constraint on translational forces and frictional torque in total shoulder arthroplasty. Clinical Orthopaedics and Related Research 29, 151–158.

Stone, K.D., Grabowski, J.J., Cofield, R.H., et al., 1999. Stress analysis of glenoid components in total shoulder arthroplasty. Journal of Shoulder and Elbow Surgery 8 (2), 151–158.

Walch, G., Edwards, T.B., Boulahia, A., et al., 2002. The Infulence of glenohumeral prosthetic mismatch on glenoid radiolucent lines: results of a multicenter study. Journal of Bone and Joint Surgery 84A, 2186–2191.

Walker, P.S., Ambarek, M.S., Morris, J.R., et al., 1995. Anterior–posterior stability in partially conforming condylar knee replacement. Clinical Orthopaedics 310, 87–97.

Wirth, M.A., Rockwood, C.A., 1996. Current concepts review: complications of total shoulder-replacement arthroplasty. Journal of Bone and Joint Surgery 78A (4), 603–616.